Supplementary Information (SI) for Journal of Materials Chemistry A.

Supporting Information

Ce single-atom synergizes icosahedral Pt_2Ce nanoparticles to promote performance enhancement for zinc-air battery

Huiqi Zhang[a], Ying Chang[a]*, Shaohong Guo[a], Yaqiong Su[b]*, Jingchun Jia[a]*, Meilin Jia[a]

a College of Chemistry and Environmental Science, Inner Mongolia Key Laboratory of Green Catalysis and Inner Mongolia Collaborative Innovation Center for Water Environment Safety, Inner Mongolia Normal University, Hohhot, 010022, China.

b School of Chemistry, Engineering Research Center of Energy Storage Materials and Devices of Ministry of Education, National Innovation Platform (Center) for Industry-Education Integration of Energy Storage Technology, Xi'an Jiaotong University, Xi'an 710049, China

**Corresponding author. E-mail: changying@imu.edu.cn, jjc1983@126.com, yqsu1989@xjtu.edu.cn*

Experimental Section

Chemicals

The chemicals required for the experiment can be used directly without further purification. $Zn(NO_3)_2 \cdot 6H_2O$ (Tianjin Guangfu Technology Development Co., Ltd., 99%), $Ce(NO_3)_3 \cdot 6H_2O$ (Adamas Reagents Co., Ltd., 99%), 2-methylimidazole (Adamas Reagents Co., Ltd., 98%), methanol (Tianjin Zhiyuan Chemical Reagent Co., Ltd., AR), ethanol (Tianjin Zhiyuan Chemical Reagent Co., Ltd., AR), KB-300 (Suzhou Yilongsheng Energy Technology Co., Ltd.), $Pt(acac)_2$ (Aladdin Reagents Co., Ltd., 97%), $Ce(acac)_3$ (Aladdin Reagents Co., Ltd., 98%), HNO_3 (Chengdu Kelong Chemical Reagents Co., Ltd., AR), H_2SO_4

(Chengdu Kelong Chemical Reagents Co., Ltd., AR), $CHCl_3$ (Chengdu Kelong Chemical Reagents Co., Ltd., AR), $Zn(OAc)_2$ (Adamas Reagents Co., Ltd., 99%), KOH (Sinopharm Chemical Reagents Co., Ltd., 90%), Nafion (Adamas Reagents Co., Ltd., 5 wt%), Pt/C (Shanghai Hesen Electric Co., 20 wt%).

Synthesis of Ce-ZIF-8

In a typical synthesis, 1.16g $Zn(NO_3)_2 \cdot 6H_2O$ (0.004 mol) and 0.18 g $Ce(NO_3)_3 \cdot 6H_2O$ (0.0004 mol) were dissolved in 30 mL of methanol, and sonicated to form a uniform mixed solution A, 2-methylimidazole was dissolved in the same volume of methanol to form solution B, solution B was poured into solution A and stirred for 6 h at room temperature, the precipitates were centrifuged and washed with methanol 3 times, and dried in vacuum at 70 ^{o}C for overnight to obtain Ce-ZIF-8.

Synthesis of CeNC

The powder of Ce-ZIF-8 was placed in a tube furnace and carbonized under flowing Ar for 2h at 900 ^{o}C with the heating rate of 5 ^{o}C min^{-1} and then naturally cooled down to room temperature to obtain the CeNC.

Synthesis of Pt_2Ce/CeNC-600

5 mg CeNC, 50 mg KB-300, 47.2 mg $Pt(acac)_2$ (0.00012 mol), 26.2 mg $Ce(acac)_3$ (0.00006 mol) were co-dissolved in 10 ml $CHCl_3$ and stirred overnight at room temperature, the product was calcined under flowing Ar for 2h at 600 ^{o}C with the heating rate of 5 ^{o}C min^{-1}. The product was post-

processed by acid etching with 0.5 M HNO_3 at 70 ^{o}C for 2 h, centrifuged and washed twice with ethanol, dried at 50^{o}C for 24 h, and finally calcined under flowing Ar for 2h at 300 ^{o}C with the heating rate of 5 ^{o}C min^{-1} to obtain Pt_2Ce/CeNC-600.

Synthesis of Pt_2Ce/C

55 mg KB-300, 47.2 mg $Pt(acac)_2$, 26.2 mg $Ce(acac)_3$ were co-dissolved in 10 ml $CHCl_3$, the remaining steps were the same as for the synthesis of Pt_2Ce/CeNC-600.

Synthesis of Pt/CeNC

5 mg CeNC, 50 mg KB-300, 70 mg $Pt(acac)_2$ were co-dissolved in 10 ml $CHCl_3$, the remaining steps were the same as for the synthesis of Pt_2Ce/CeNC-600.

Characterizations

The morphology of the samples were observed by field emission scanning electron microscopy (SEM, Germany-Zeiss-GeminiSEM 360 and USA-FEI-Quanta FEG 250 + Oxford Energy Spectroscopy) and field emission transmission electron microscopy (TEM, Japan-JEOL-JEM-2100F). Spherical aberration corrected transmission electron microscopy (AC-STEM) were taken on a USA-Thermo Fisher Scientific-Titan Themis G2 60-300. The structure and crystallinity were investigated by X-ray diffraction (XRD, Germany-Bruker-D8 ADVANCE and Rigaku Ultima IV). The chemical composition and electronic valence states were analyzed by X-ray photoelectron spectroscopy (XPS, USA-Thermo SCIENTIFIC ESCALAB 250Xi). X-ray absorption spectroscopy (XAS) measurements and data analyses were performed at Beijing Synchrotron Radiation-Absorption Spectroscopy XAFS (EXAFS+XANES).

Electrochemical ORR analysis

The tests were performed with a AutoLab electrochemical workstation and a rotating disk electrode device. The tests were performed using a three-electrode system, with the rotating disk electrode (RDE) and the rotating ring-disk electrode (RRDE) as the working electrodes (WE), the Ag/AgCl electrode as the reference electrode (RE) and the platinum wire as the counter electrode (CE). 0.5 M H_2SO_4 was used as the electrolyte, prior to testing, 30 min of O_2 or Ar was passed through the electrolyte to remove the impurity gases from the electrolyte. Preparation of catalyst ink: dissolve 2 mg of catalyst powder in 400 μL mixed solution (V_{Nafion}: V_{DI}: $V_{ethanol}$ = 1:9:10), and ultrasonicate for 30 minutes to ensure the solution is thoroughly mixed. Before the ORR test, 16μL catalyst slurry was coated on the working electrode. For ORR, the Pt loadings on the electrode of Pt_2Ce/CeNC-600 and Pt/C are 88.4 and 81.6 μg/cm^2. Tests included cyclic voltammetry (CV), linear sweep voltammetry (LSV), transfer electron number, hydrogen peroxide yield and accelerated durability test (ADT). The CV potential was in the range of -0.2-1 V with a sweep rate of 100 mV/s. The LSV potential was in the range of -0.2-1 V with a sweep rate of 10 mV/s, and the curves under oxygen atmosphere are 2500, 2025, 1600, 1225, 900 and 625 rpm. The ADT is the change in LSV before and after 1000 CV cycles. All potentials were converted versus reversible hydrogen electrode (RHE) with the equation:

$$E_{RHE} = E_{Ag/AgCl} + (0.197 + 0.0591\,pH)\,V$$

The electron transfer number (n) for ORR was determined using Koutecky-Levich (K-L) analysis (equation (1)):

$$\frac{1}{j} = \frac{1}{j_{\mathrm{L}}} + \frac{1}{j_{\mathrm{K}}} = \frac{1}{B\omega^{\frac{1}{2}}} + \frac{1}{j_{\mathrm{K}}} \qquad (1)$$

where j, j_K and j_L represent measured, kinetic, and diffusion-limited current densities, respectively. j_K is a constant at a certain potential and j_L is proportional to the square root of angular velocity (ω) of the rotation disk electrode. The proportionality coefficient (B) is given by equation (2):

$$B = 0.62nFC_0D_0^{2/3}v^{-1/6} \qquad (2)$$

where n is the number of electrons transferred in the ORR, F is the Faraday constant (96,485C mol^{-1}), C_0 is the bulk concentration of O_2 (1.1×10^{-3} mol cm^{-3}), D_0 is the diffusion coeffcient of O_2 (1.93×10^{-5} cm^2 s^{-1}), and v is the kinematic viscosity of the electrolyte (0.01 cm^2 S^{-1}).

H_2O_2 yield:

$$H_2O_2\% = 200 \times \frac{\frac{I_R}{N}}{I_D + \frac{I_R}{N}} \qquad (3)$$

Electron transfer number：

$$n = 4 \times \frac{I_D}{I_D + \frac{I_R}{N}} \quad (4)$$

Where I_R represents the ring current, I_D represents the disk current, and N is the current collection efficiency of Pt ring electrode.

Zinc air battery testing

A polished metallic zinc foil (6.5 cm × 1 cm × 0.3 mm) was used as the anode, a carbon paper-nickel foam composite loaded with Pt_2Ce/CeNC-600 was used as the air cathode, and the electrolyte was a mixed solution containing 6 M KOH, 0.2 M $Zn(OAc)_2$ and 500 ml ultrapure water. Preparation of catalyst ink: dissolve 5 mg of catalyst powder in 1000 μL mixed solution (V_{Nafion}: V_{DI}: $V_{ethanol}$ = 1:9:10), and ultrasonicate for 30 minutes to ensure the solution is thoroughly mixed. Prepare a 3.5 cm × 6.5 cm carbon paper-nickel foam composite, at the center point (1 cm × 1 cm), evenly apply 200 μL of catalyst ink in four separate applications and allow it to dry. The Pt loadings on the carbon paper-nickel foam composite of Pt_2Ce/CeNC-600 and Pt/C are 216.7 and 200.0 μg/cm^2. The discharge polarization curves and power density curves of the cells were tested using CHI 760E. The discharge curves at different current densities and galvanostatic discharge-charge cycle profiles of the battery were tested using LAND CT2001A. A complete charge-discharge cycle takes 20 min.

Computational details

All calculations were performed using the plane-wave periodic DFT method in the Vienne ab initio simulation package (VASP). The electron energies used the generalized gradient approximation in the Perdew-Burke-Ernzerhof (GGA-PBE). The projector augmented wave (PAW) method is used to describe the electron-ion interaction. The cutoff energy was set as 400 eV to ensure the accurate energies. The Gaussian electron smearing method is used by $\sigma = 0.05$ eV. The DFT lattice parameters for the Graphite bulk are a=2.459 Å, b=2.459 Å, c=6.800 Å, The surface of (001) was modeled by periodic slabs with $p(6\times6)$ unit cell. The vacuum layer was set as 12 Å to avoid interactions with other slabs. A 3 × 3 × 1 Monkhorst-Pack k-point grid was used for sampling the Brillouin zone. The geometry optimization was done when the energy difference was lower than 10^{-4} eV and the convergence criterion on forces smaller than 0.05 eV/Å.

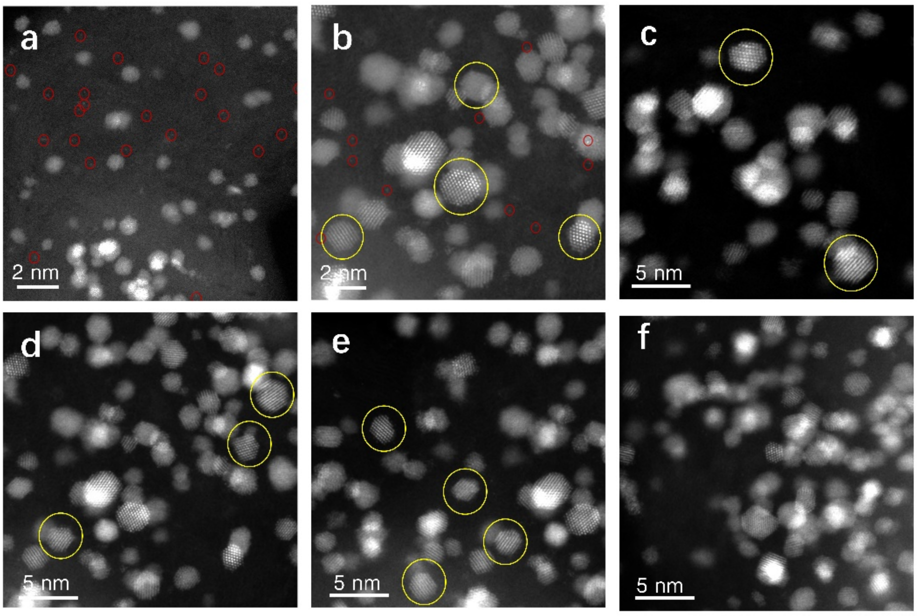

Supplementary Figures

Figure S1. AC-STEM images of Pt_2Ce/CeNC-600.

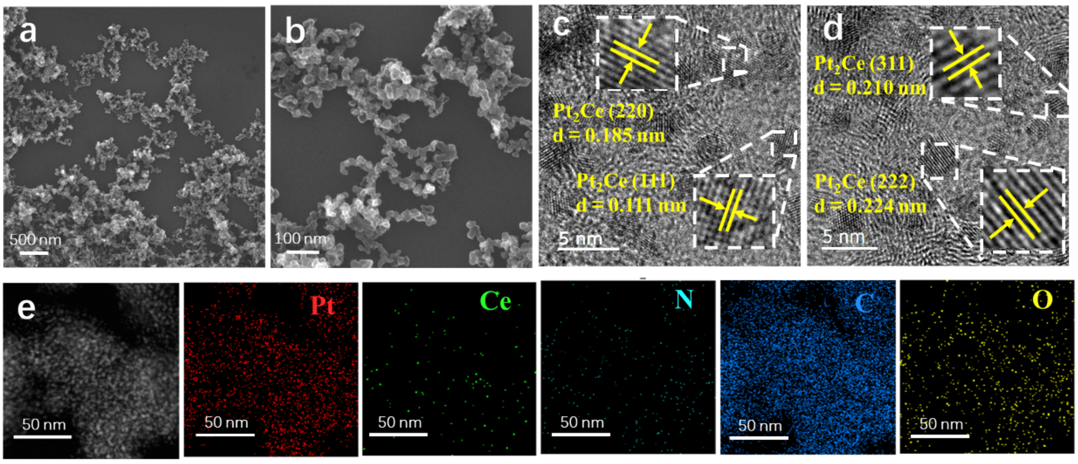

Figure S2. (a, b) SEM images of Pt_2Ce/CeNC-600. (c, d) HRTEM images of Pt_2Ce/CeNC-600. (e) HAADF-STEM corresponding to EDS mapping for Pt_2Ce/CeNC-600.

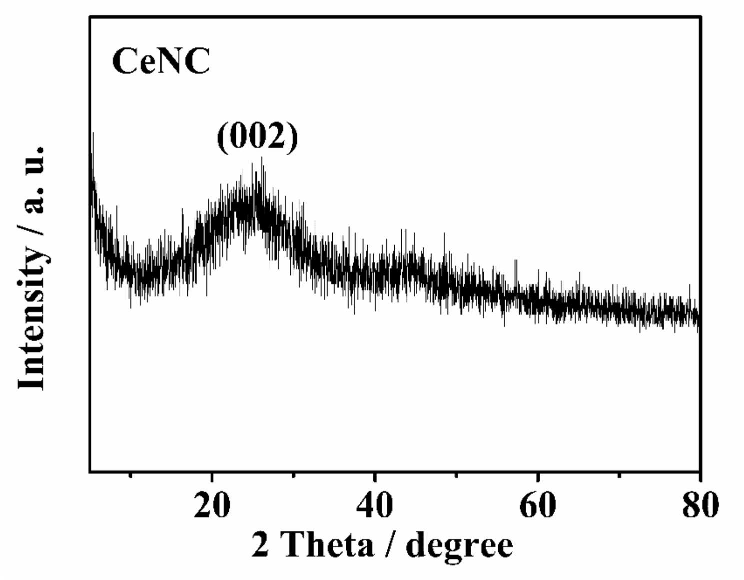

Figure S3. XRD of CeNC.

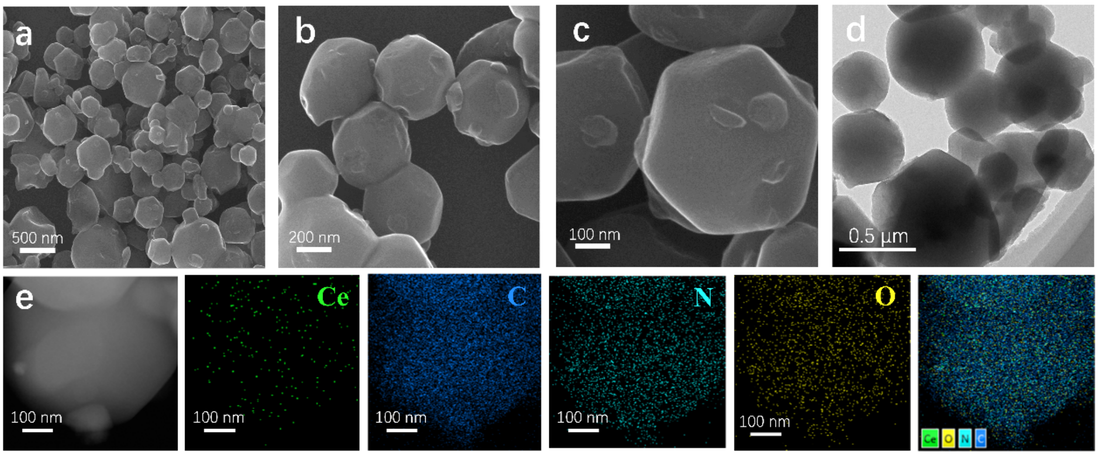

Figure S4. (a, b, c) SEM images of CeNC. (d) TEM image of CeNC. (e) HAADF-STEM corresponding to EDS mapping for CeNC.

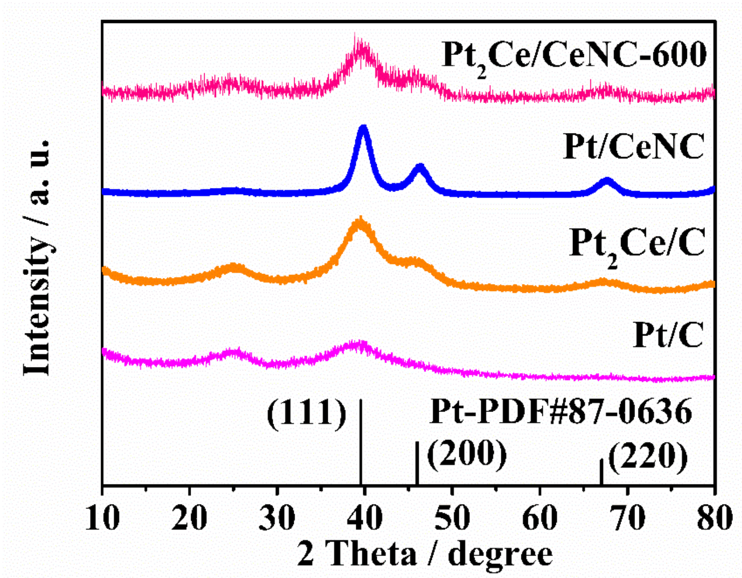

Figure S5. XRD of Pt_2Ce/CeNC-600, Pt/CeNC, Pt_2Ce/C and Pt/C.

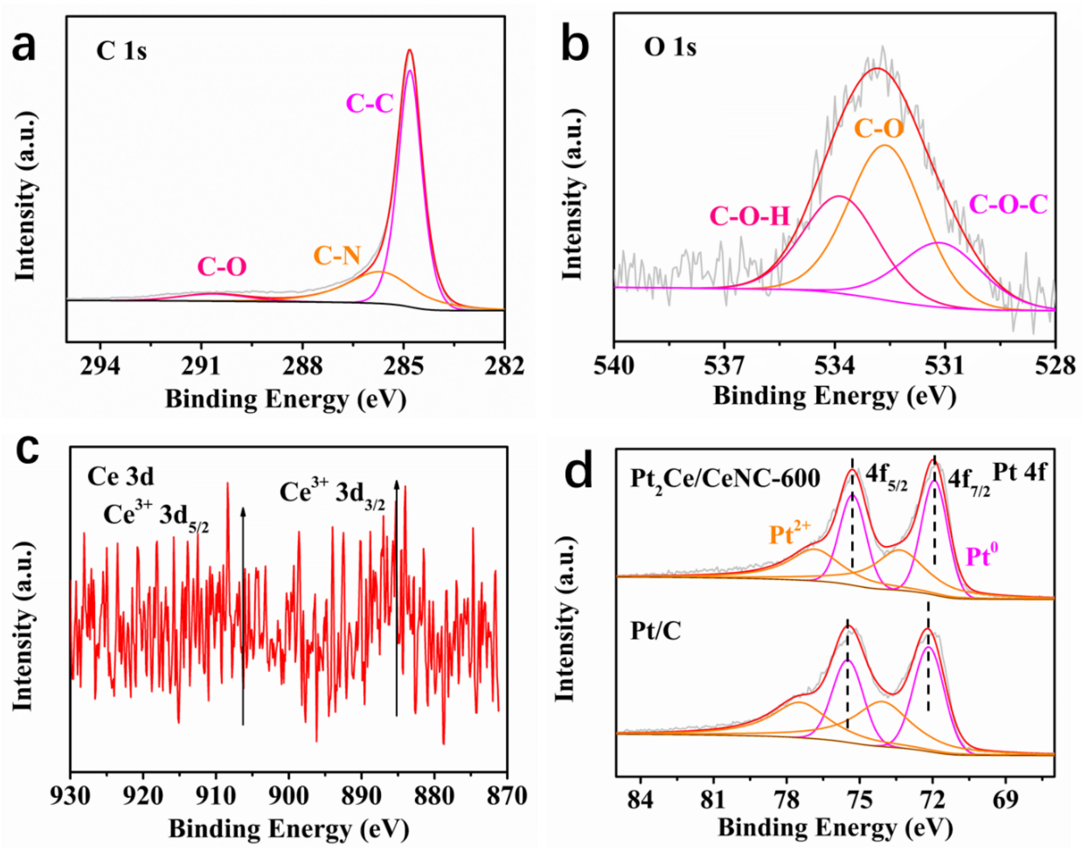

162 **Figure S6.** (a) C 1s XPS spectra of Pt_2Ce/CeNC-600. (b) O 1s XPS
163 spectra of Pt_2Ce/CeNC-600. (c) Ce 3d XPS spectra of Pt_2Ce/CeNC-600.
164 (d) Pt 4f XPS spectra of Pt_2Ce/CeNC-600 and Pt/C.

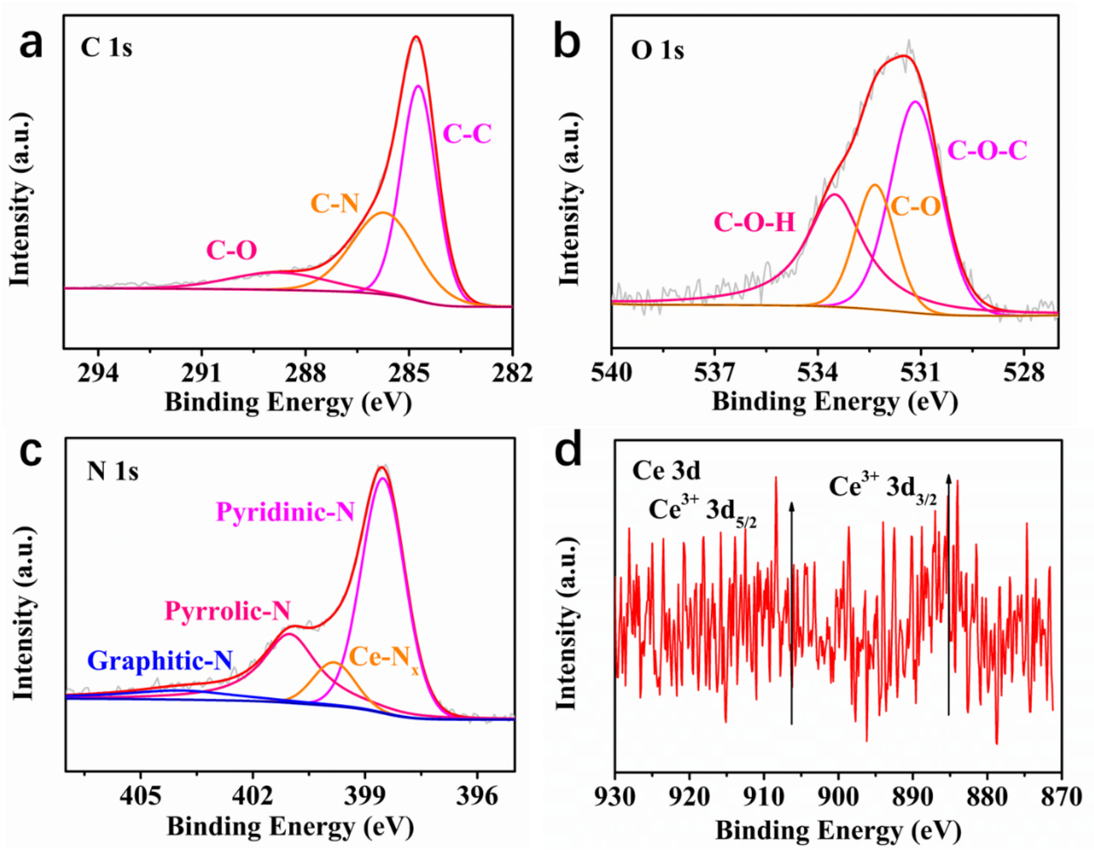

166 **Figure S7.** XPS spectra of CeNC. (a) C 1s XPS spectra. (b) O 1s XPS

167 spectra. (c) N 1s XPS spectra. (d) Ce 3d XPS spectra.

168

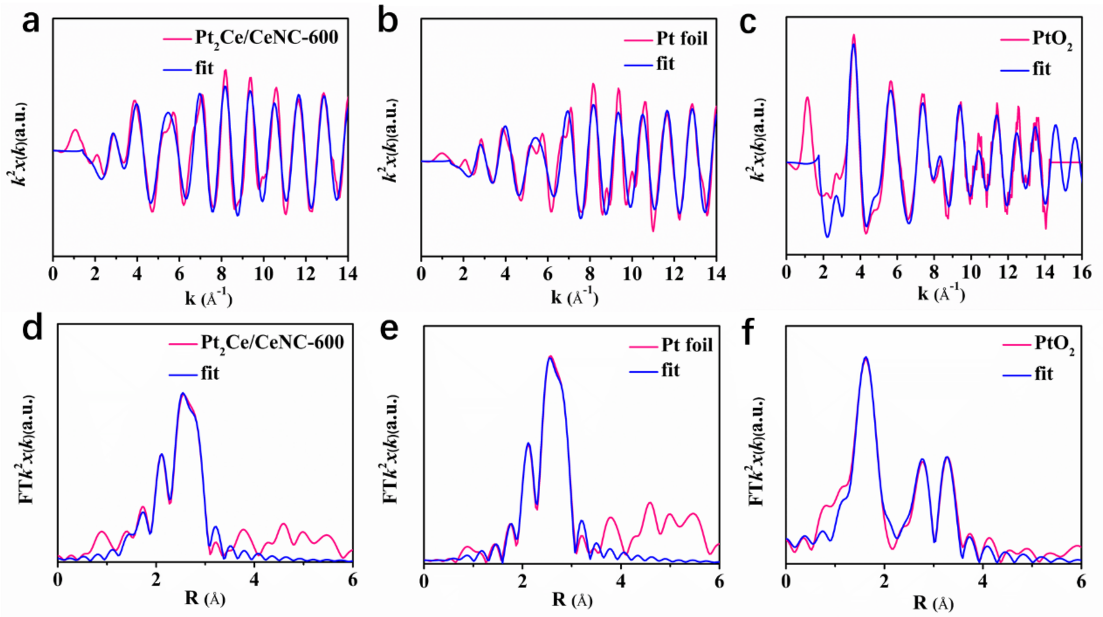

Figure S8. (a) k space FT-EXAFS fitting curves of Pt_2Ce/CeNC-600. (b) k space FT-EXAFS fitting curves of Pt foil. (c) k space FT-EXAFS fitting curves of PtO_2. (d) R space FT-EXAFS fitting curves of Pt_2Ce/CeNC-600. (e) R space FT-EXAFS fitting curves of Pt foil. (f) R space FT-EXAFS fitting curves of PtO_2.

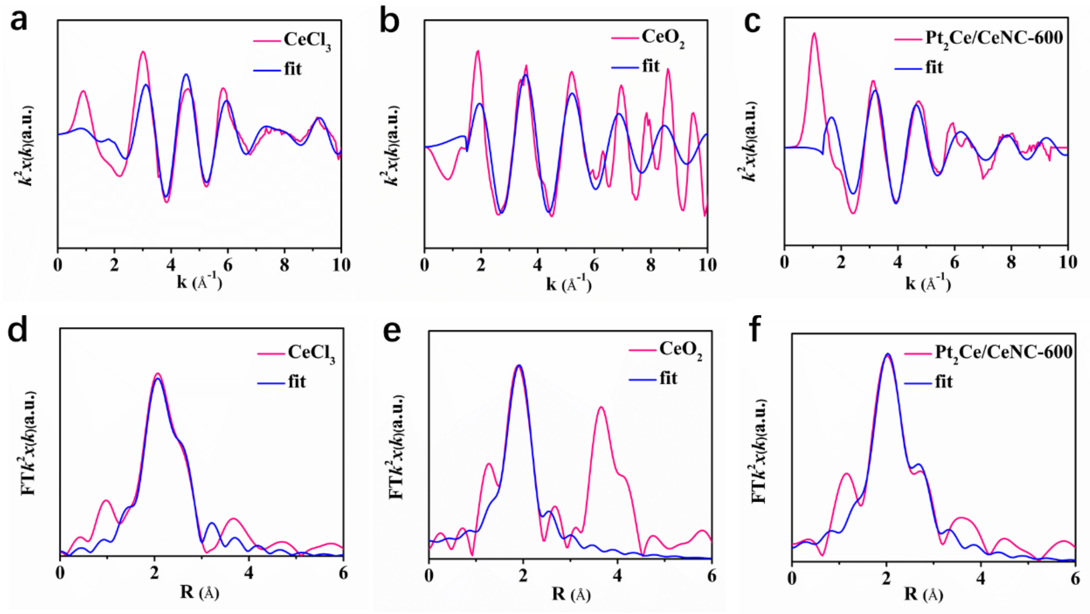

Figure S9. (a) k space FT-EXAFS fitting curves of $CeCl_3$. (b) k space FT-EXAFS fitting curves of CeO_2. (c) k space FT-EXAFS fitting curves of Pt_2Ce/CeNC-600. (d) R space FT-EXAFS fitting curves of $CeCl_3$. (e) R space FT-EXAFS fitting curves of CeO_2. (f) R space FT-EXAFS fitting curves of Pt_2Ce/CeNC-600.

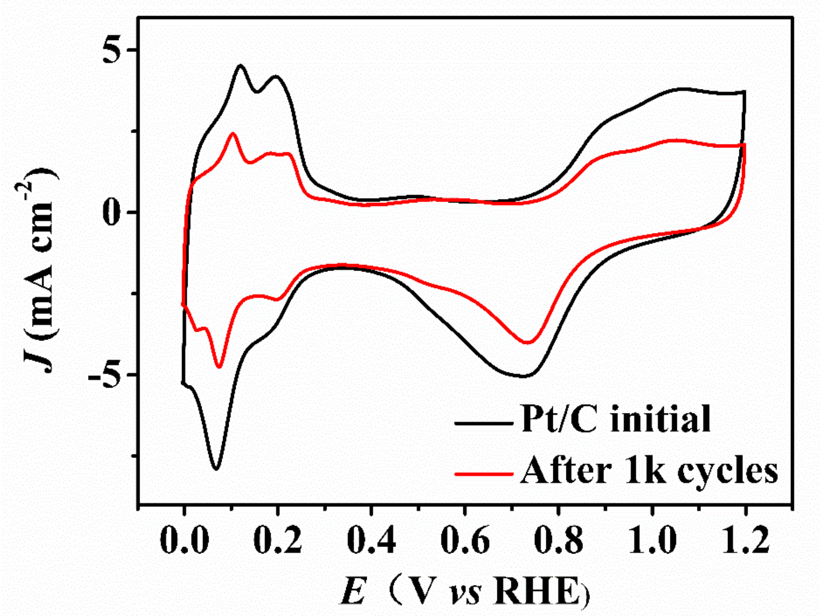

181 **Figure S10.** CV of Pt/C after 1k cycles.

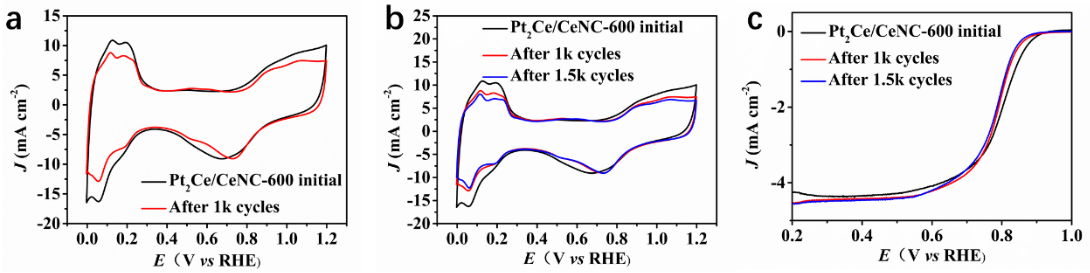

Figure S11. (a) CV of Pt_2Ce/CeNC-600 after 1k cycles. (b) CV of Pt_2Ce/CeNC-600 after 1.5k cycles. (c) Durability test of Pt_2Ce/CeNC-600 for 1.5k cycles.

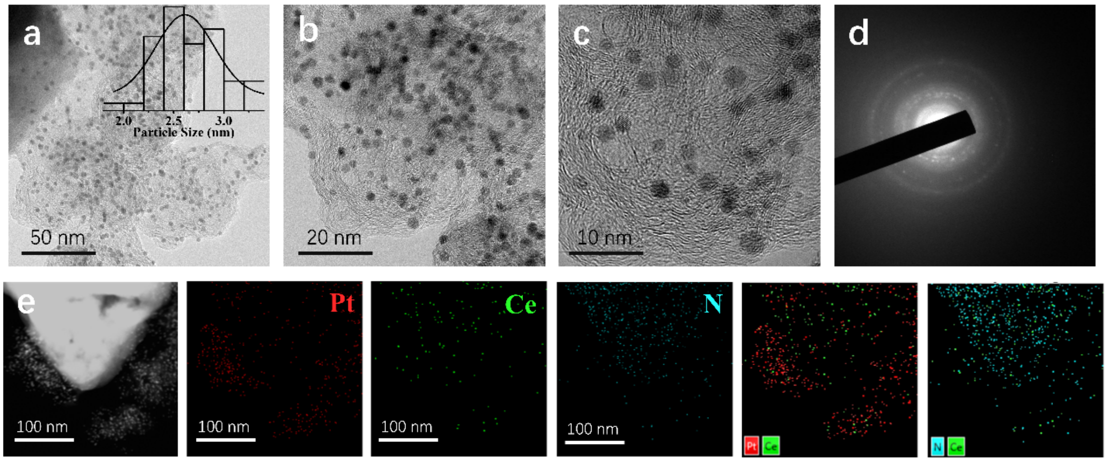

Figure S12. (a, b, c) TEM images of Pt_2Ce/CeNC-600 after durability test. The inset of (a) is histogram of particle size distribution of Pt_2Ce/CeNC-600 after durability. (d) SAED. (e) HAADF-STEM corresponding to EDS mapping for Pt_2Ce/CeNC-600 after durability.

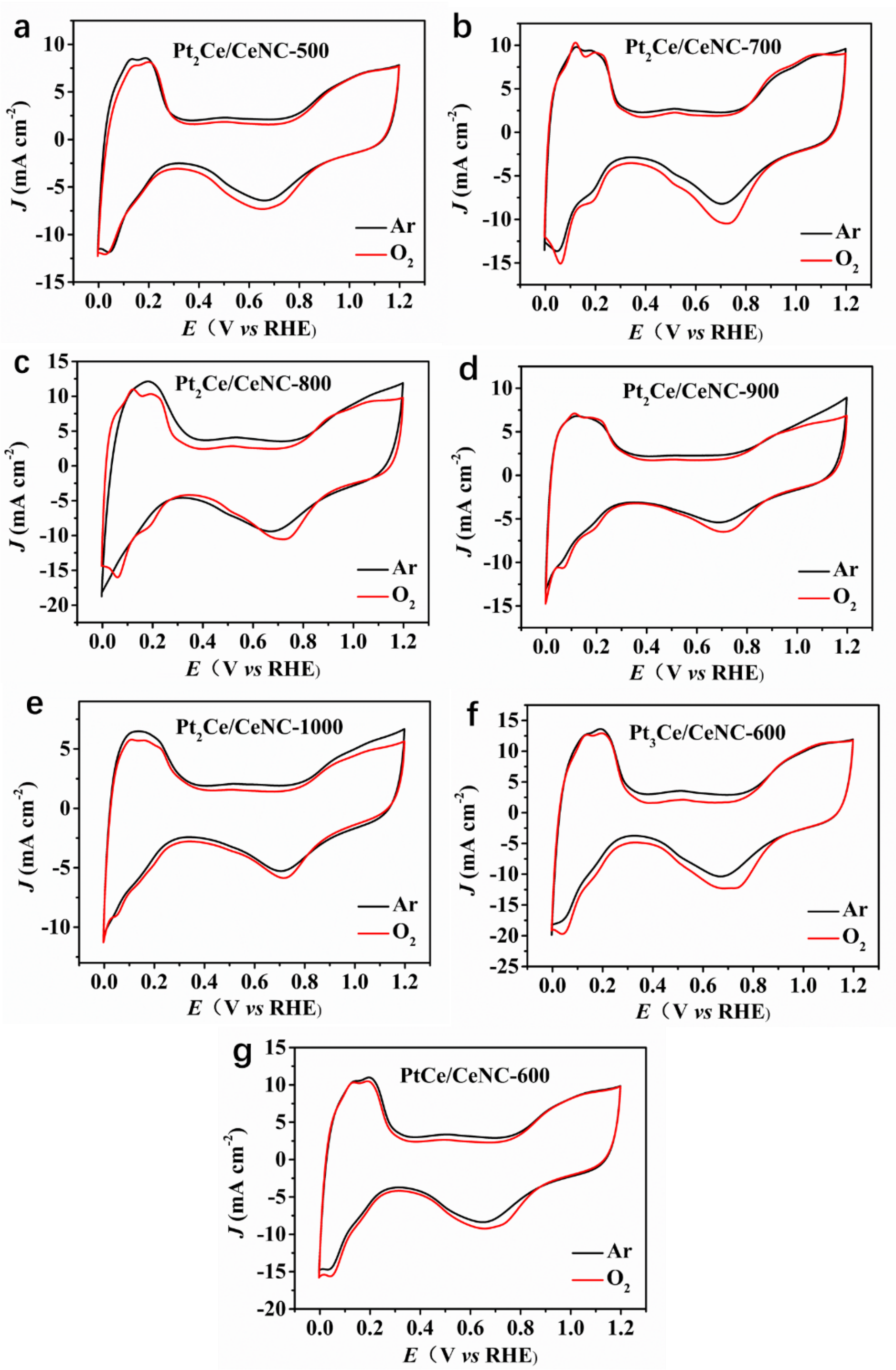

Figure S13. CV of all comparative samples.

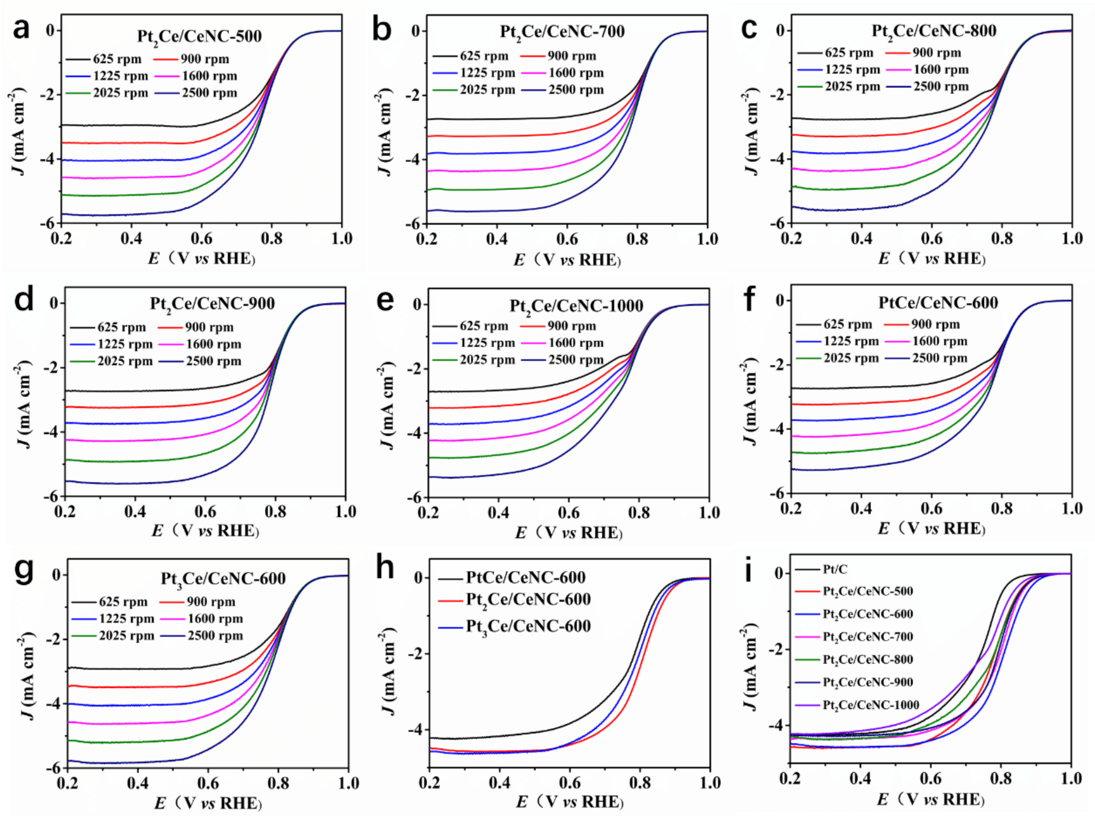

Figure S14. LSV of all comparative samples.

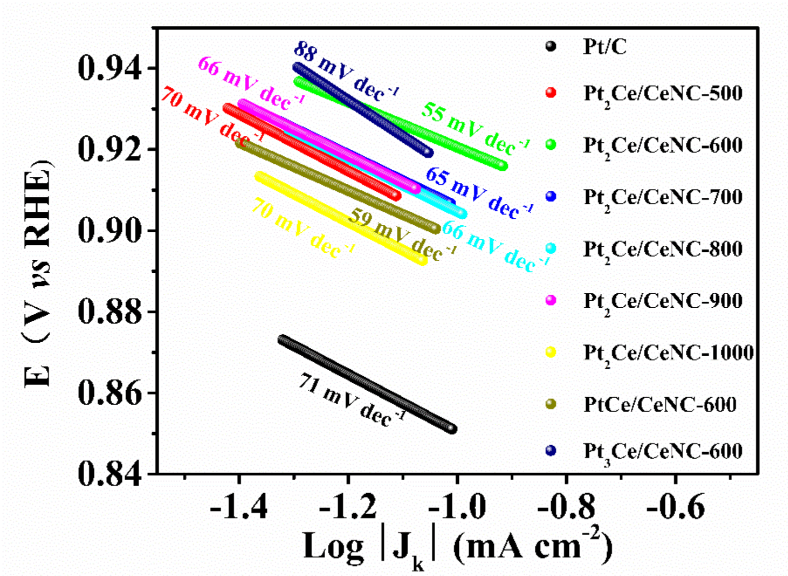

Figure S15. Tafel plots of all comparative samples.

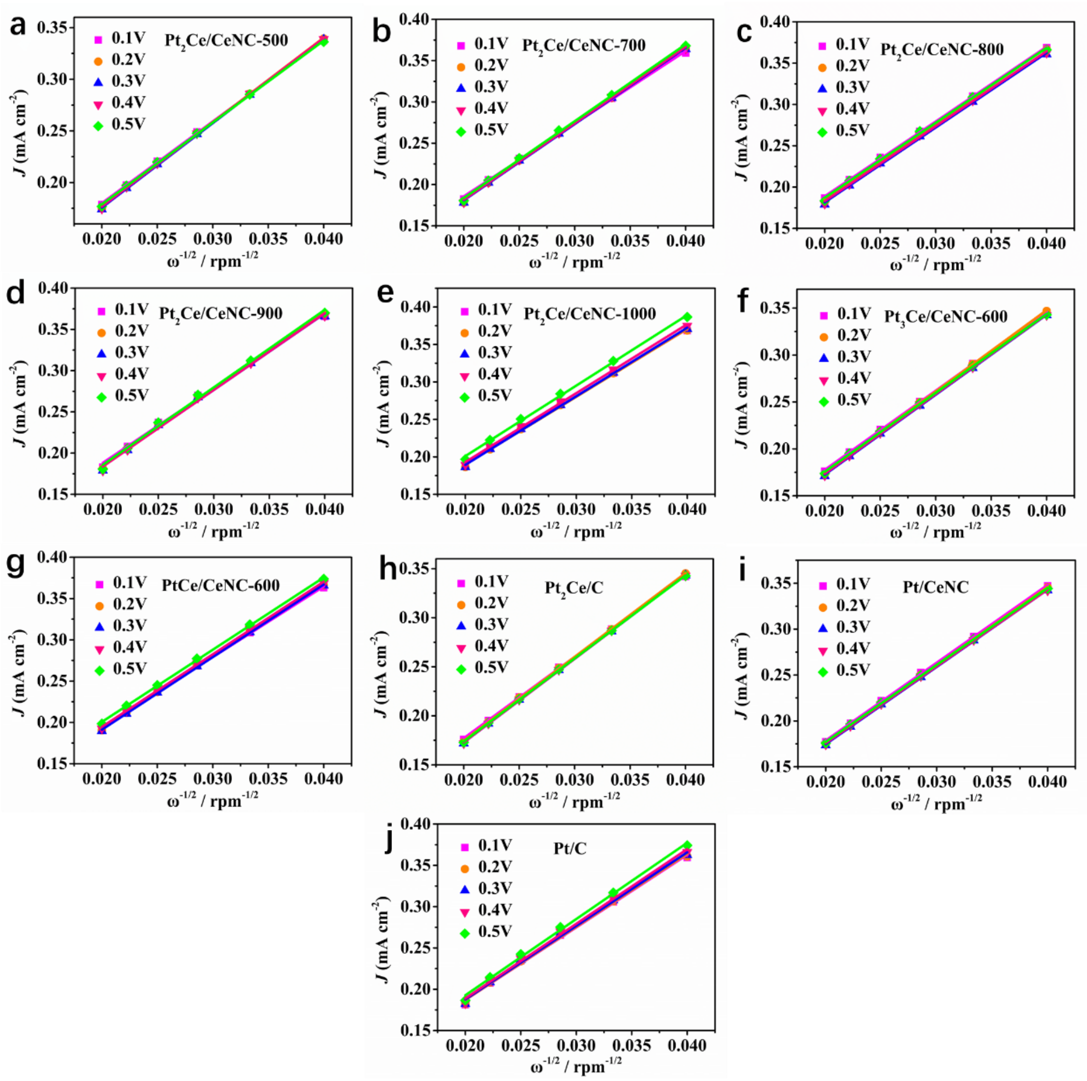

Figure S16. K-L equation of all comparative samples.

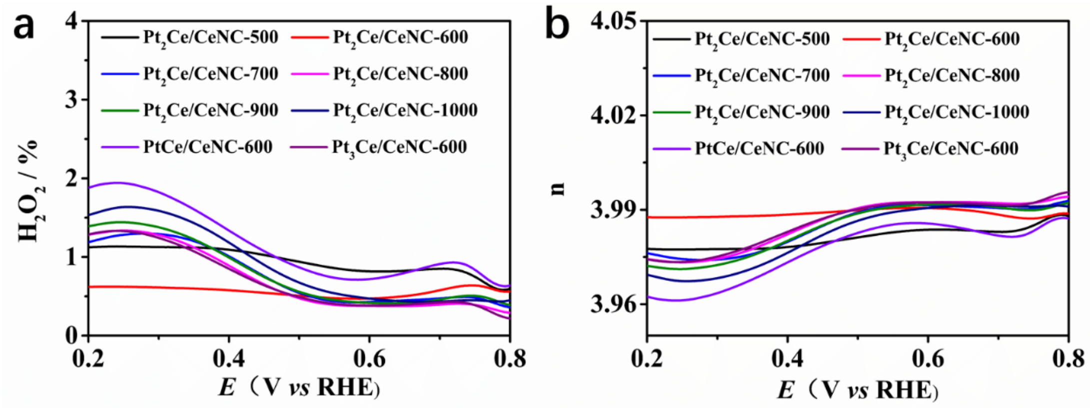

Figure S17. (a) H_2O_2 yield of all comparative samples. (b) Electron-transfer number of all comparative samples.

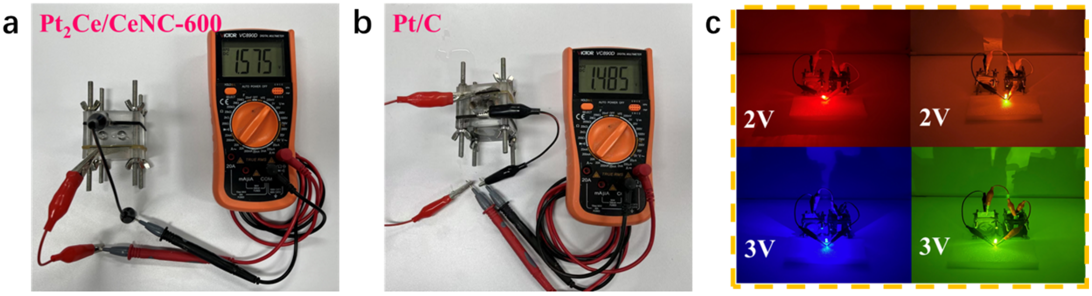

Figure S18. (a) Open-circuit voltage of Pt_2Ce/CeNC-600. (b) Open-circuit voltage of Pt/C. (c) Photograph of lighting a light-emitting diode (2.0–3.0 V) by connecting two Pt_2Ce/CeNC-600 based ZABs in series.

Table S1. Elemental composition of the Pt_2Ce/CeNC-600 measured by ICP-MS.

Catalysts	Pt (wt. %)	Ce (wt. %)
Pt_2Ce/CeNC-600	21.67%	0.14%